Parallel Beam Propagation Method for the Analysis of Second Harmonic Generation

Husain M. Masoudi and John M. Arnold

Abstract— **We extend the linear parallel Explicit Finite-Difference Beam Propagation Method to model the nonlinear second harmonic generation process in three-dimensional waveguides. It has been concluded from testing this method that it is accurate as well as very efficient.**

I. Introduction

THE Explicit Finite-difference Beam Propagation Method (EFD-BPM) is a very efficient BPM for analysing linear optical devices [1]–[3]. In previous work we showed that the parallel version of this method is several times faster than the parallel Real Space (RS-BPM) method [2]–[3]. The BPM has been used, in both finite-difference [4] and FFT [5] forms, to study two-dimensional Second Harmonic Generation (SHG). In addition, it has been applied to three dimensional SHG with circular geometry (optical fibers) under the approximation that the fundamental field is undepleted, using again the finite-difference form [6]. In this letter we apply the EFD-BPM to analyse full three-dimensional optical devices that contain a second order nonlinearity $\chi^{(2)}$, using two different parallel machines. It has been observed that the method can model large complicated optical structures very efficiently due the speed of the parallel implementations. To validate the results of the method, two numerical examples are given and the results are compared with the existing 1-D coupled mode analysis [7]–[9].

II. Numerical Method

Considering the coupled parabolic wave equations in three-dimension for both the fundamental and the second harmonic waves subject to a homogeneous second order nonlinearity $\chi^{(2)} = \chi^{(2)}(2\omega;\omega,\omega) = \chi^{(2)}(\omega;2\omega,-\omega)/2$

$$2jk_0n_0\frac{\partial E^f}{\partial z} = \frac{\partial^2 E^f}{\partial x^2} + \frac{\partial^2 E^f}{\partial y^2} + k_0^2(n_f^2 - n_0^2)E^f + k_0^2\chi^{(2)}E^sE^{f*} \quad (1a)$$

$$4jk_0n_0\frac{\partial E^s}{\partial z} = \frac{\partial^2 E^s}{\partial x^2} + \frac{\partial^2 E^s}{\partial y^2} + 4k_0^2(n_s^2 - n_0^2)E^s + 2k_0^2\chi^{(2)}E^fE^f \quad (1b)$$

Manuscript received August 16, 1994; revised November 21, 1994.

Husain M. Masoudi is with the Department of Electronics and Electrical Engineering, University of Glasgow, Glasgow G12 8LT UK, on leave from King Fahd University of Petroleum and Minerals, Department of Electrical Engineering, Dhahran 31261, Saudi Arabia.

John M. Arnold is with the Department of Electronics and Electrical Engineering, University of Glasgow, Glasgow G12 8LT, UK.

IEEE Log Number 9409024.

where E^f and E^s are the fields of the fundamental and the second harmonic respectively. Throughout this work, subscripts or superscripts for both f and s are related to the fundamental wave and the second harmonic wave respectively, n_0 is a reference refractive index for the problem and k_0 is the free space wave number at the fundamental frequency defined as $k_0 = 2\pi/\lambda_f$. With little modification to (1), two different n_0's for the two fields could be chosen, with values close to the values of the effective indices of the two fields; this will lead to a more accurate representation to (1). However, in this work n_0 is chosen as a common value equal to the substrate refractive index of the waveguide, which is also close to the two effective indices of the two waves. Applying the central finite-difference approximation to (1) will give the following SHG Explicit Finite-Difference BPM (SHG-EFD-BPM) [1]–[3]

$$E^f_{i,m}(z+\Delta z) = E^f_{i,m}(z-\Delta z) + d_x[E^f_{i+1,m}(z) + E^f_{i-1,m}(z)] + d_y[E^f_{i,m+1}(z) + E^f_{i,m-1}(z)] + b_f E^f_{i,m}(z) + \alpha E^s_{i,m}(z)E^{f*}_{i,m}(z) \quad (2a)$$

$$E^s_{i,m}(z+\Delta z) = E^s_{i,m}(z-\Delta z) + \frac{d_x}{2}[E^s_{i+1,m}(z) + E^s_{i-1,m}(z)] + \frac{d_y}{2}[E^s_{i,m+1}(z) + E^s_{i,m-1}(z)] + b_s E^s_{i,m}(z) + \alpha E^f_{i,m}(z)E^f_{i,m}(z) \quad (2b)$$

where $b_r = [\Delta z/(jn_0k_r)][-2/(\Delta x^2) - 2/(\Delta y^2) + k_r^2(n_r^2 - n_0^2)]$, $r = f$ or s, $k_0 = k_f = k_s/2$, $d_\rho = -j\Delta z/(n_0k_0\Delta\rho^2)$, $\alpha = \Delta z k_0\chi^{(2)}/(jn_0)$ and $\rho = x$ or y. i and m represent the discretization of both the fundamental and the second harmonic fields and of the refractive indices with respect to the transverse directions x and y respectively. Δz is a small step in the direction of propagation z.

We have developed two parallel computer codes for the SHG-EFD-BPM which run on a 64-transputer array and a Connection Machine (CM-200), using the same techniques as in [2]–[3]. The implementation of the SHG-EFD-BPM on the transputer array has been done by dividing the transverse mesh points of the discretised fundamental field into 2-D equal blocks of data where each block is assigned to one processor of the 2-D topology of the transputer array. The same has been done for the second harmonic transverse field using the same 2-D topology of the fundamental field computations. In other words, each processor computes the local computational block data of both the fundamental and the second harmonic fields

and they exchange only values at the local border points at the edges of the blocks with neighboring processors. On the other hand, the implementation of the SHG-EFD-BPM on the CM is almost identical to our linear one in [3]; first the fundamental field at $z + \Delta z$ is computed, then the second harmonic field at $z + \Delta z$ is computed, where all the field points are operated on concurrently using a single instruction. Numerical tests for the SHG-EFD-BPM showed that the method is stable for a propagational step Δz very close to the values of the linear counterpart in [1]–[3]; this is due to the small effect of the last term on the right hand side of (2) on the stability when $\chi^{(2)}$ is very small (practical values are in the range of 10^{-12} m/V).

In order to validate the results of the SHG-EFD-BPM we have also implemented the following one dimensional coupled wave equations using the fourth order Runge-Kutta method (Ψ represents the 1-D field) [7]–[10]:

$$\frac{d\Psi^f}{dz} = -j\frac{k_0\chi^{(2)}}{2n_f^{\text{eff}}}\Psi^s\Psi^{f*}e^{-j\Delta k' z},$$
$$\frac{d\Psi^s}{dz} = -j\frac{k_0\chi^{(2)}}{2n_s^{\text{eff}}}\Psi^f\Psi^f e^{j\Delta k' z} \tag{3}$$

where the wave vector mismatch is $\Delta k' = 2k_0(n_s^{\text{eff}} - n_f^{\text{eff}})$. The 1-D equation in (3) is similar to the 3-D equation in (1), with the transverse variations projected onto modes. This can be derived from (1) by writing the fields in (1) as a projection of the z-dependent fields (1-D) onto the corresponding 3-D eigenfunctions ϕ^f and ϕ^s (the mode distributions). Multiplying (1a) by ϕ^f and (1b) by ϕ^s and integrating over the cross sectional area (A) of the device, will lead to (3). The relationships between the 1-D and the 3-D fields, can be expressed from the power relation ($P = [n\Psi^2/(2Z_0)]A_{\text{eff}}, Z_0$ is the free space impedance) where

$$A_{\text{eff}} = \left(\int\int_A \phi^f dA\right)^2 \left(\int\int_A \phi^s dA\right) \Big/ \left[\int\int_A (\phi^f)^2\phi^s dA\right]^2 \tag{4}$$

The full derivation of the above can be found in [10]. For perfect phase matching ($\Delta k' = 0$) (3) leads to the well known solutions for the normalized intensities of $I^f/I_0 = \text{sech}^2(\Gamma z)$ and $I^s/I_0 = \tanh^2(\Gamma z)$, where $\Gamma = k_0\chi^{(2)}|\Psi_0^f|/2\sqrt{n_f^{\text{eff}}n_s^{\text{eff}}}$, and I_0 and Ψ_0^f are the initial intensity and field of the fundamental respectively.

Example 1: The first numerical test for the parallel SHG-EFD-BPM involves a nearly perfect phase-matched waveguide. The rib waveguide in Fig. 1 has been used with the following parameters (all dimension are in μm): $\lambda_f = 1.55$, $\lambda_s = 0.775$, $n_{gf} = 3.44$, $n_{gs} = 3.4062406$, $n_{\text{sub}} = 3.34$, $\chi^{(2)} = 300$ pm/V. In this example, n_{gs} is chosen such that the two modes' effective indices are equal. Using $\Delta x = \Delta y = 0.1$ μm and equal lengths of 8 μm for the x and y window sizes, the computed first guided mode effective indices of both fields, using $\Delta z = 0.025$ and $n_0 = n_{\text{sub}}$, are $n_f^{\text{eff}} = 3.39236226$ and $n_s^{\text{eff}} = 3.39236228$. For simplicity zero boundary conditions at the edges of the computational window have been used. Fig. 2 shows the normalized intensity of both the fundamental and the second harmonic versus the longitudinal distance z (μm), where the first guided mode of the fundamental waveguide is used as an input and zero initial field is assumed for the second harmonic waveguide. In the same figure we have included the solution of (3) for comparison, using an effective area (computed from (4)) of the 3-D fields of 1.896 μm^2. Clearly, the figure shows the excellent agreement of the two results.

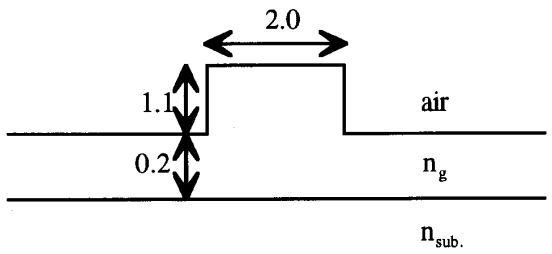

Fig. 1. The rib waveguide used in the computations.

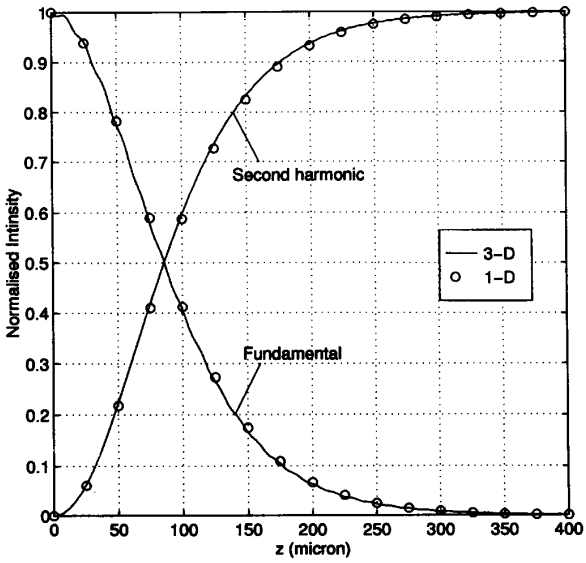

Fig. 2. The normalized intensity of a phased matched waveguide (Example 1) for both the fundamental and the SHG versus the longitudinal distance z (μm), using the parallel SHG-EFD-BPM (3-D) and the solution of (3) (1-D), with an input power = 27.2 W.

Example 2: The second numerical test involves a nonphase-matched process using the same waveguide of the first example with following alterations (the parameters of this example are chosen to match real values [9]): $n_{\text{sub}} = 3.4$, $n_{gf} = 3.5$, $n_{gs} = 3.6$. The computed first guided mode effective indices of both fields are $n_f^{\text{eff}} = 3.45299169$ and $n_s^{\text{eff}} = 3.58591145$ where the computed effective area of the fields is 1.92 μm^2. In practice, Quasi Phase Matching (QPM) for the parallel SHG-EFD-BPM can be achieved by introducing gratings during the propagation to change the relative phase difference between the two fields. The BPM mismatch wave vector is defined as $\Delta k = \beta_s^p - 2\beta_f^p - 2\pi/\Lambda$, where β_f^p and β_s^p are the parabolic wave vector of both the fundamental and the second harmonic fields, and Λ is the grating period length. It is

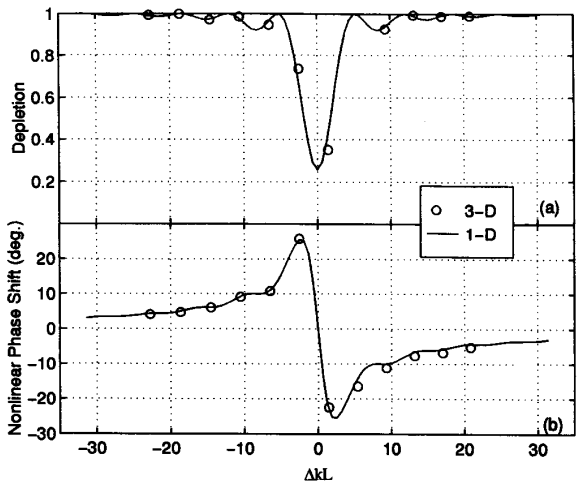

Fig. 3. The results of a non-phased-matched waveguide (Example 2) for both of the parallel SHG-EFD-BPM (3-D) and the 1-D Runge–Kutta with an input power = 4.9 W (with $\Delta k'L = \Delta kL$). (a) The normalized depletion of the fundamental intensity as a function of ΔkL. (b) The nonlinear phase shift $\theta_{\rm NL}$ as a function of ΔkL.

known that the effective nonlinearity of the QPM interaction is $2/\pi$ smaller than the ordinary phase matched interaction with reversed nonlinear domains [7]. In this example, the first guided mode of the fundamental waveguide has been propagated, using the parallel SHG-EFD-BPM, to a distance of $L = 1$ mm with a QPM grating along the propagation direction. The grating used in the computations is a rectangular wave such that the second order nonlinear coefficient $\chi^{(2)}$ has either its full value or zero in alternate half-periods of the grating; in this case the effective nonlinearity is reduced by $1/\pi$ [7]. For the 1-D case of (3), there are two methods to simulate QPM technique using the solution of (3). The first method is to use exactly the same procedure of the 3-D BPM with actual structural periodic gratings for the second order nonlinear coefficient $\chi^{(2)}$ along the z direction, and the second method (the one implemented in this work) is to reduce the value of the $\chi^{(2)}$ by the QPM factor $1/\pi$, while changing explicitly $\Delta k'$ to $\Delta k' = 2k_0(n_s^{\rm eff} - n_f^{\rm eff}) - 2\pi/\Lambda$, in (3), to simulate the existence of second-order nonlinear gratings [10]. Fig. 3 shows the results of both the parallel SHG-EFD-BPM and the solution of (3) (Runge-Kutta) with $\Delta z = 0.01$ for both methods. We compute the output depletion and nonlinear phase change of the fundamental field for different grating lengths, assuming that the phase of fundamental field (3-D) is changing as $e^{-j(\beta_f^p z + \theta_{\rm NL})}$ where $\theta_{\rm NL}$ is the nonlinear phase shift of the fundamental field. The figure shows that the parallel SHG-EFD-BPM results are very close to the 1-D coupled mode predictions of (3). Finally, the total execution time for each run of example 2 is around 10.3 min on the CM-200 using 16 k processors and around 76.3 min using 64 processors of the transputer array; these are more than twice the time of the linear parallel EFD-BPM in [2]–[3].

In conclusion we have shown the implementations of the previous parallel EFD-BPM using two parallel machines in the nonlinear domain with a second order nonlinearity $\chi^{(2)}$. Two simple tests of the algorithm showed that the method is very reliable and very efficient for the analysis of complicated three-dimensional nonlinear optical devices.

ACKNOWLEDGMENT

Mr. Masoudi gratefully acknowledges the support of King Fahd University of Petroleum and Minerals (Saudi Arabia) while he is at the University of Glasgow.

REFERENCES

[1] Y. Chung and N. Dagli, "Analysis of Z-Invariant and Z-Variant semiconductor rib waveguides by explicit finite difference beam propagation method with nonuniform mesh configuration," *IEEE J. Quant. Elect.*, vol. 27, pp. 2296–2305, 1991.

[2] H. M. Masoudi and J. M. Arnold, "Parallel beam propagation methods," *IEEE Photon. Technol. Lett.*, vol. 6, pp. 848–850, July 1994.

[3] H. M. Masoudi and J. M. Arnold, "Parallel three-dimensional finite-difference beam propagation methods," *Int. J. Num. Mod.*, in press.

[4] G. Krijnen, H. Hoekstra, and P. Lambeck, "BPM simulations of integrated optic structure containing second order nonlinearity," *ECIO (Euro. Conf. Intg. Opt.)*, 5-4 to 5-5, 1993.

[5] B. Hermansson and D. Yevick, "A propagation beam method analysis of nonlinear effects in optical waveguides," *Opt. Quant. Elect.*, vol. 16, pp. 525–534, 1984.

[6] P. Weitzman and U. Osterberg, "A modified beam propagation method to model second harmonic generation in optical fibers," *IEEE J. Quant. Elect.*, vol. 29, pp. 1437–1443, 1993.

[7] M. Fejer, G. Magel, D. Jundt, and R. Byer, "Quasiphase matched second harmonic generation: Tuning and tolerances," *IEEE J. Quant. Elect.*, vol. 28, pp. 2631–2654, 1992.

[8] R. DeSalvo, D. Hagan, M. Sheikh-Bahae, G. Stegeman, and E. Stryland, "Self-focusing and self-defocusing by cascaded second-order effects in KTP," *Opt. Lett.*, vol. 17, pp. 28–30, 1992.

[9] C. Ironside, J. Aitchison, and J. Arnold, "An all-optical switch employing the cascaded second-order nonlinearity effect," *IEEE J. Quant. Elect.*, vol. 29, pp. 2650–2654, 1993.

[10] H. M. Masoudi and J. M. Arnold, "Modeling second-order nonlinear effects in optical waveguides using a parrallel-processing beam propagation method," *IEEE J. Quant. Elect.*, submitted.